Changes in density of states caused by chemisorption*

Theodore L. Einstein†
Department of Physics, University of Pennsylvania, Philadelphia, Pennsylvania 19174
(Received 23 January 1975)

The process of chemisorption is studied via the change in density of states ($\Delta\rho$) when an adatom with a single level E_a bonds by a hopping parameter V to the (100) surface of an s-band simple cubic crystal. As V increases, the bond changes from a perturbative regime to the formation of a surface complex. Investigations of local and layer-summed $\Delta\rho$ show this dimerlike structure to be well localized near the bond. Steric effects (binding-site symmetry) are easily introduced. A damping parameter can be added to simulate decay effects of surface probes. Application of the model to photoemission angular-averaged and angular-resolved difference spectra for light gases on tungsten gives understanding of the bonding peak near the bottom of the band, of the depletion of states near the Fermi energy, and of the slight shifting of the energy-momentum-conserving peak.

I. INTRODUCTION

To gain insight into the complex process of chemisorption, it has been necessary and often desirable to deal with simple models. The natural approach from chemistry is to replace the substrate by a small cluster of atoms, and then to apply extended Hückel,[1] complete neglect of differential overlap[2] (CNDO), scattered-wave $X\alpha$,[3] or some other scheme. From the opposite vantage of free-electron metal physics, the natural procedure is to represent the substrate by semi-infinite jellium,[4] thereby losing, at least to lowest order, any aspect of graininess in the bulk. A third viewpoint, rooted in studies of transition metals, treats the substrate in the tight-binding model representing the metallic wave functions as linear combinations of atomic orbitals. Usually the basis is limited to spherically symmetric (s-band) orbitals, and often the real bcc or fcc structure is simplified to a chain[5,6] or a simple cubic (sc) lattice.[7,8]

In this paper we shall focus on the last-mentioned type of substrate, the (100) surface of a single s-band simple-cubic semi-infinite lattice in the tight-binding approximation. Since its (100) surface lattice structure is square, like a (100) bcc or fcc structure, it should give an especially reasonable accounting of chemisorption when the binding perturbation is localized at the top layer. The physical process we envision is the adsorption of a light gas atom (H, O, N, C, etc.) on a transition-metal surface. To extract information from our model, we shall calculate chemisorption-induced changes in local and total electronic density of states (DOS). We shall demonstrate in detail the conveniences afforded by the simplifications of our model, in particular how several of the summations involved in calculating (the initial-state aspect of) photoemission spectra reduce to geometric series, which can be summed by hand. In the next generalization, s-band fcc or bcc crystals, such analytic summations would not be possible; moreover, the replication of realistic clean-surface DOS curves is no better than the simple-cubic results, and in many ways worse. On the other hand, we can compute factors which are intrinsically absent in chain models, such as dependence on adatom binding site and, as was discussed in an earlier paper[8] (hereafter referred to as ES), the indirect interaction between pairs of adatoms.

To be explicit, the (100) sc lattice model for the substrate is that which has been treated by Kalkstein and Soven[9] and Allan.[7] The tight-binding method employed is known to give a better idea of the narrow-band properties of transition metals than electron-gas models. The one-center tight-binding parameter is set to zero, thereby establishing the center of the bulk band as the zero of energy. The two-center tight-binding matrix element $-T$ sets the energy scale and gives a bandwidth W_b of $12T$.

We shall take $T=\frac{1}{2}$, giving a bandwidth of 6. We represent the adatom by a single nondegenerate (excepting spin) level of energy E_a. The best rough estimate of E_a is the (negative) average of the ionization (I) and affinity (A) levels, which usually sits around the center of the d-band rather than near its bottom. The model is most realistic for neutral adsorption, i.e., when E_a is near the Fermi energy, and when the Coulomb interaction ($\sim I-A$) is not too large.

Following Grimley,[10] Newns,[6] Allan,[7] Penn *et al.*,[11] and ES,[8] we consider adatom-substrate binding from the standpoint of the Anderson model.[12] In particular, an electron on the adatom (called a) can hop to only the adatom's nearest neighbor (called 1) on the surface—or to its two four nearest neighbors in the case of bridge (centered) binding.

From a chemist's viewpoint, our model is an infinite three-dimensional Hückel model, with the

Coulomb integral α being 0 for the substrate and the resonance integral β being $-T$. The adatom α' is E_a, while β' is $-V$, where β' is the resonance term between the adatom and its nearest bulk neighbor(s). Steric effects enter naturally, since the adatom can sit above a substrate site (A or atop) or symmetrically between two (B or bridge) or four (C or centered). As suggested earlier, Hückel models traditionally are applied to small clusters. One then diagonalizes the Hamiltonian matrix and solves for eigenvectors. For an infinite system, however, the matrix becomes infinite, and there are an infinite number of eigenstates. Thus, even if one could write down any eigenvector—as one can for a clean semi-infinite s-band substrate using symmetry and other general arguments—the useful quantity is the distribution of these states in energy and space, i.e., the DOS.

In Sec. II we shall study the formalism of the calculation, displaying the appropriate Green's functions. In addition to detailed work on the change in DOS ($\Delta\rho$), we shall derive expressions for the initial-state effects of angular-resolved photoemission, and show how the separable and geometric series that arise for a (100) sc lattice simplify the computations. The reader who is primarily concerned with results can turn directly to Sec. III, which presents our results, some of which were sketched in a previous letter.[13] We depict the changes in total and local DOS, discussing steric effects, and then simplifying to atop binding. We show how the surface complex limit of binding gives a low-lying peak and a depletion of states within the band. These results are brought to bear on both angular-averaged and angular-resolved photoemission difference spectra. We can gain some understanding of the coarse structure and one source of (some of) the fine structure. We also see clearly the dominating extra structure produced by momentum-conserving transitions in the angular-resolved case. Section IV presents a brief summary and discusses how self-consistency and multiadatom effects will modify the simple picture presented.

II. FORMAL DEVELOPMENT

Since our relatively simple model has been previously discussed by Allan[7] and by ES (using the same notation as here), we merely recapitulate the key results. The perturbation term in the Hamiltonian, which produces binding to the surface, connects only sites a and 1; hence the total change in DOS when V is "turned on" is[7,8]

$$\Delta\rho(E) = \pi^{-1}\,\mathrm{Im}\left(\frac{\partial}{\partial E}\right)\ln[1 - V^2 G_{aa}(E) G_{11}(E)] , \quad (2.1)$$

where $G = (E - H - i\delta)^{-1}$ is the advanced Green's function for the dissociated ($V = 0$) system. In the future we shall neglect energy arguments when no confusion is possible. The form of the perturbation Hamiltonian also simplifies the Dyson equation for $\mathcal{G}$, the advanced Green's function for the perturbed (bound) system. After a bit of easy algebra, we find

$$\mathcal{G}_{aa} = G_{aa}/(1 - V^2 G_{aa} G_{11}) , \quad (2.2a)$$

$$\mathcal{G}_{ia} = \mathcal{G}_{ai} = -V \mathcal{G}_{aa} G_{1i} , \quad (2.2b)$$

$$\mathcal{G}_{ij} = G_{ij} + \mathcal{T} G_{1i} G_{1j} , \quad (2.2c)$$

where $\mathcal{T} = V^2 \mathcal{G}_{aa}$ is the 11 component of the T matrix. Equation (2.2c) shows that $\Delta\mathcal{G}_{ij} \equiv \mathcal{G}_{ij} - G_{ij}$ depends on i and j only through G_{1i} and G_{1j} separately, so that any double sum distributes into the product of two single sums. Finally we find the decomposition relating Eq. (2.1) to Eq. (2.2):

$$\Delta\rho = \sum_{\mu} \Delta\rho_{\mu\mu} , \quad (2.3)$$

where μ includes the adatom as well as the substrate sites, denoted by Roman subscripts.

Characterizing the adatom by a single energy level leads to the simple expressions

$$G_{aa} = (E - E_a - i\delta)^{-1} ;$$
$$\mathcal{G}_{aa} = [E - E_a - V^2 G_{11}(E) - i\delta]^{-1} . \quad (2.4)$$

Since experiments measure the difference between chemisorbed systems and clean substrates, the quantity of real interest is

$$\Delta\tilde{\rho}(E) = \Delta\rho(E) + \delta(E - E_a)$$
$$= \frac{1}{\pi}\,\mathrm{Im}\frac{\partial}{\partial E}\ln[E - E_a - V^2 G_{11}(E) - i\delta] . \quad (2.5)$$

For weak V the self-energy term will be important only near E_a, by replacing $G_{11}(E)$ by $G_{11}(E_a)$ we obtain Grimley's[10] virtual-level approximation. For very strong V, the argument of the ln in Eq. (2.5) can be replaced by just $G_{11}(E)$, which is the expression obtained in creating a vacancy at site 1. In this regime we also find the possibility of a zero of the ln argument below and also above the band; these are the well-known split-off states.[5,6,8,10]

As in ES, we shall use a (100) s-band simple-cubic lattice as our substrate,[14] expanding on the treatment (and computer program) of Kalkstein and Soven (KS).[9] Since two-dimensional periodicity is preserved under crystal cleavage, KS chose a mixed Bloch-Wannier representation. Then

$$G_{ij} = N_{\parallel}^{-1} \sum_{\vec{k}_{\parallel}} e^{i\vec{k}_{\parallel}\cdot(\vec{R}_i - \vec{R}_j)} G(n_i, n_j; \vec{k}_{\parallel}) , \quad (2.6)$$

where n_i labels the layer, zero being the surface layer. For the infinite crystal,

$$G^0(n, n'; \vec{k}_{\parallel}) = G^0(n - n'; \vec{k}_{\parallel})$$

by translation symmetry. KS show

$$G^0(n;\vec{k}_{\parallel}) = (i/\mu)(-\omega - i\mu)^{|n|}\ , \tag{2.7a}$$

where the nearest-neighbor hopping is $-\frac{1}{2}$,

$$\omega = E + \cos k_x d + \cos k_y d \tag{2.7b}$$

(d being the lattice constant) and

$$\mu = |1-\omega^2|^{1/2} \times \begin{cases} 1\ , & \text{if } \omega^2 \le 1 \\ i\omega/|\omega|\ , & \text{if } \omega^2 > 1 \end{cases}\ . \tag{2.7c}$$

KS cleave the crystal by applying a perturbation to cancel electron hopping between planes $n=0$ and $n=-1$. Alternatively,[15,16] one could erect an infinite diagonal potential on plane $n=-1$. In either case, the resulting Dyson's equation leads to

$$\begin{aligned} G(m,n;\vec{k}_{\parallel}) &= (i/\mu)[(-\omega - i\mu)^{|m-n|} - (-\omega - i\mu)^{m+n+2}] \\ &= G^0(|m-n|;\vec{k}_{\parallel}) - G^0(m+n+2;\vec{k}_{\parallel}) \end{aligned} \tag{2.8}$$

and, in particular, using $\omega^2 + \mu^2 = 1$,

$$G(0,n;\vec{k}_{\parallel}) = -2(-\omega - i\mu)^{n+1}\ . \tag{2.9}$$

Equation (2.9) is particularly fortunate, since a sum over $G(0,n)$ reduces to a geometric series.

Finally, it is valuable to know the moments of the DOS[17,18] of a (100) sc lattice

$$\mu_n \equiv \pi^{-1} \int_{-3}^{3} (E')^n \,\mathrm{Im} G(E')\, dE'\ , \tag{2.10}$$

especially to locate the splitoff-state energies, since outside the band

$$\mathrm{Re}G(E) = \frac{1}{E}\sum_{n=0}^{\infty} \frac{\mu_n}{E^n}\ , \quad |E| > 3\ . \tag{2.11}$$

For R_i and R_j of Eq. (2.5) both in the surface layer and with a difference vector $(pd,\ qd,\ 0)$, we have shown that the only nonvanishing moments have the value

$$\begin{aligned} \mu_{2m+p+q} = [(-1)^{p+q}/2^{2m+p+q}] &\binom{2m+p+q}{m+p} \\ &\times \sum_{l=0}^{m} \binom{2l+p+q}{l} \binom{m+p}{m-l} \binom{m+q}{m-l} \Big/ (m-l+1) \end{aligned} \tag{2.12}$$

for non-negative integers $m,\ p,\ q$.[19]

As an example of the simplifications afforded by a (100) sc lattice, we consider the sum of the changes within a single layer,

$$\Delta\rho_m = \pi^{-1}\,\mathrm{Im} \sum_{j\in m} \mathcal{T} G_{j1}^2\ . \tag{2.13}$$

Inserting Eq. (2.6), then performing the layer sum in j first, using the evenness in $\vec{k}_{\parallel}$ and Eq. (2.9), finally doing one of the $\vec{k}_{\parallel}$ sums, we find

$$\begin{aligned} \Delta\rho_m &= \pi^{-1}\,\mathrm{Im}\mathcal{T} N_{11}^{-1} \sum_{\vec{k}_{\parallel}} G(0,m;\vec{k}_{\parallel})^2 \\ &= -(2/\pi)\,\mathrm{Im}\mathcal{T} G_{1M}\ , \end{aligned} \tag{2.14}$$

where site M is directly beneath site 1 (and the adatom) in the $2m+1$ layer. Thus, the computer effort required to obtain $\Delta\rho_m$ is no greater than that to find a single $\Delta\rho_{jj}$, viz., a two-dimensional sum over the surface Brillouin zone.

A major application of our formalism is a study of the initial-state effects of photoemission, in particular the difference spectra (chemisorbed minus clean). The process we envision is a photon of energy $\hbar\omega$ exciting an electron of energy E (measured relative to the band center) to a final plane-wave state $|p\rangle$ of momentum p and energy $E_p = p^2/2m$. Thus E_p is measured relative to the inner potential (or relative to the vacuum level if one neglects the inner potential, as we shall do for simplicity). We denote by E_c the difference the energy zero of E_p and the center of the band. Obviously this scenario glosses over the important multiple-scattering effects in the final state; these have been discussed, and examined closely for a (100) s-band simple cubic lattice, by Liebsch.[20]

The interaction Hamiltonian for the photon absorption[21] is the electric-dipole term $(e/mc)\vec{p}\cdot\vec{A}$, where we do not have to be careful about symmetrized ordering since $\vec{A}$ can be taken with vanishing divergence. By the golden rule, the rate is

$$\left(\frac{e}{mc}\right)^2 \sum_i |\langle \vec{p}|\vec{p}\cdot\vec{A}|i\rangle|^2 \delta(E_{\vec{p}} - \hbar\omega + E_c - E_i)\ , \tag{2.15}$$

where $|p\rangle$ is the final plane-wave eigenstate and $|i\rangle$ the initial states expressed as linear combinations of the Bloch-Wannier basis states. The sum over i of the linear coefficients times the δ function is just $\pi^{-1}\,\mathrm{Im}G$, so the rate can be written

$$\left(\frac{e\vec{p}\cdot\vec{A}}{mc}\right)^2 \sum_{\mu,\nu} \tilde{\varphi}_{\mu}(\vec{p})\tilde{\varphi}_{\nu}^*(\vec{p})\rho_{\mu\nu}(E)\, e^{-i\vec{p}\cdot(\vec{R}_{\mu}-\vec{R}_{\nu})}\ , \tag{2.16}$$

where $\tilde{\varphi}(p)$ is the Fourier transform of a single substrate orbital. If all the orbitals are identical, the orbital factors can be taken out of the summation. If not, the summation can be broken up into parts having the same orbitals. While the orbital effects are sometimes non-negligible,[22] we shall represent the change in rate from a surface due to adsorption of a single adatom by

$$\sum_{\mu,\nu} \Delta\tilde{\rho}_{\mu\nu}(E)\, e^{-i\vec{p}\cdot(\vec{R}_{\mu}-\vec{R}_{\nu})}\ . \tag{2.17}$$

As in Eq. (2.5), the tilda indicates that the isolated adatom should not be included in nonadsorbed systems, as in the experimental realization.

Two sorts of photoemission measurements are generally made: angular averaged and angular resolved. In the angular-averaged setup, one tries

to collect all electrons emerging in the hemisphere above the sample. The theoretical counterpart is a hemispherical average over the angular factor in the exponent of (2.17). By the inversion symmetry of almost all substrates, the hemispherical average is just half the spherical average (i.e., the $\mu\nu$ contribution from the omitted hemisphere equals the $\nu\mu$ contribution from the included hemisphere, since $\Delta\rho_{\mu\nu}$ is symmetric in its indices). If $\chi_{\mu\nu}$ denotes $p|\vec{R}_\mu - \vec{R}_\nu|$, then we find that the spherical average of the exponential term in (2.44) is $\chi_{\mu\nu}^{-1}\sin\chi_{\mu\nu}$. Taking as a model system 21.2-eV photons impinging on tungsten, we estimate $\chi_{\mu\nu}$ to be of order 9 for nearest neighbors. However, although the angular factor drops by an order of magnitude in going from a diagonal ($\chi_{\mu\mu}$) to a nearest-neighbor term, this diminuation is partially compensated by the presence of several equivalent (four for bulk simple cubium) nearest neighbors. On the other hand, succeeding neighbors will tend to interfere and cancel the extrema of the nearest-neighbor contribution. It is thus a qualitatively very reasonable but quantitatively tentative approximation to represent change in rate by $\Delta\tilde{\rho}$. In the angular-averaged case, the neglect of orbital factors is especially inconsequential. This factor would merely contribute a monotonic envelope varying by of order 2 over the energy range of interest.[22]

An obvious way to account for damping in Δj—the change in photoemission yield due to the adsorption of one adatom—is to sum the $\Delta\rho$'s in each plane and weight this subtotal with a damping factor:

$$\Delta j \propto \rho_{aa} + \sum_{m=0} \Delta\rho_m e^{-\lambda m} . \tag{2.18}$$

Using the geometric nature of $G(0, n)$ [Eq. (2.9)], we can simplify Eq. (2.18) as we did Eq. (2.14):

$$\sum_m \Delta\rho_m e^{-\lambda m} = -\frac{2}{\pi}\mathrm{Im}\mathcal{T}N_{\|}^{-1}\sum_{k_{\|}} \frac{G(0, 1; \vec{k}_{\|})}{1 + \frac{1}{2}G(0, 1; \vec{k}_{\|})\, e^{-\lambda}} . \tag{2.19}$$

We easily check that Eq. (2.19) is correct in the two extreme limits of λ: for $\lambda = \infty$ we get a contribution from only the top layer. In Eq. (2.19) the denominator reduces to unity, and summation becomes just $\Delta\rho_0$ of Eq. (2.14). For $\lambda = 0$ or $e^{-\lambda} = 1$, the summand reduces (using $\omega^2 + \mu^2 = 1$) to $i(-\omega - i\mu)/\mu$. Further manipulation (note $\partial\mu/\partial E = -\omega/\mu$) shows that this is just $\frac{1}{2}\partial G(0, 0; k_{\|})/\partial E$. Performing the $k_{\|}$ sum then essentially reproduces the substrate contribution to the total $\Delta\rho$ [cf., Eq. (2.3)]. We again see that the time to compute the Δj for arbitrary λ is no greater than that to compute a single-substrate Green's function, viz., a summation over the surface Brillouin zone (i.e., just one-eighth of it, by symmetry). Alternatively, since the $\Delta\rho_m$ converge fairly rapidly, one can just compute the first several, and then do the layer sum explicitly for various values of λ. In general, λ should be energy and angle dependent. In view of the relative crudeness of going from Eq. (2.17) to (2.18), these effects should be negligible, at least for a first view.

In angular-resolved photoemission, one focuses on a particular direction of $\vec{p}$ in Eq. (2.17). Equation (2.17) decomposes naturally into three pieces:

$$\frac{d\Delta j}{d\Omega} \propto I_a + I_{ab} + I_b , \tag{2.20}$$

where I_a, I_b, and I_{ab} are the contributions from the adatom, the substrate, and their interference, respectively. Obviously I_a is just ρ_{aa}. If we define

$$S(p, E) \equiv \sum_j G_{ij}(E)\, e^{-i\vec{p}\cdot\vec{R}_j} , \tag{2.21}$$

then using the separability property of Eq. (2.2c), we find

$$I_b = \pi^{-1}\,\mathrm{Im}[\mathcal{T}S(\vec{p}, E)S(-\vec{p}, E)] , \tag{2.22}$$

and with Eq. (2.2b),

$$I_{ab} = -\pi^{-1}\,\mathrm{Im}\{(\mathcal{T}/V)[S(\vec{p}, E)\, e^{i\vec{p}\cdot\vec{R}_a} + S(-\vec{p}, E)\, e^{-i\vec{p}\cdot\vec{R}_a}]\} . \tag{2.23}$$

For a (100) sc lattice, $S(p, E)$ is particularly easy:

$$S(\vec{p}, E) = \sum_n e^{-ip_\perp na} \sum_{j\in n} e^{-i\vec{p}_{\|}\cdot\vec{R}_j} N_{\|}^{-1} \sum_{\vec{k}_{\|}} G(0, n; \vec{k}_{\|})\, e^{i\vec{k}_{\|}\cdot\vec{R}_j} . \tag{2.24}$$

Here we have decomposed the j sum into a subsum within layer n and then a sum over layers. In writing G_{1j}, we have taken R_1, the substrate site nearest the adatom, to be the origin. Performing the $j\in n$ sum first dictates that $\vec{p}_{\|}$ must equal $\vec{k}_{\|}$ up to a reciprocal-lattice vector. Since G depends on $\vec{k}_{\|}$ only through ω, and ultimately cosine terms [cf., Eq. (2.7)], we have a built-in extended-zone formalism and do not have to translate explicitly $\vec{p}_{\|}$ to the first-surface Brillouin zone. Using Eq. (2.9), we have

$$S(\vec{p}, E) = \sum_{n=0} e^{-ip_\perp na}(-2)(-\omega - i\mu)^{n+1}\big|_{\vec{p}_{\|}} . \tag{2.25}$$

To account for damping, we can place an additional factor of $e^{-\lambda n}$ under the summation. Since Eq. (2.25) is a geometric series, it sums easily to

$$S(\vec{p}, E) = \frac{G(0, 0; \vec{p}_{\|})}{1 + \frac{1}{2}G(0, 0; \vec{p}_{\|})\, e^{-ip_\perp a}\, e^{-\lambda}} . \tag{2.26}$$

If we recall that ω (and hence G) is even in $p_{\|}$, and if we define

$$\mathfrak{D}_\lambda(\vec{p}, E) = \frac{2(\omega + i\mu)}{[1 + (\omega + i\mu)\, e^{-ip_\perp a}\, e^{-\lambda}][1 + (\omega + i\mu)\, e^{+ip_\perp a}\, e^{-\lambda}]}$$

then we can simplify Eqs. (2.22) and (2.23) by writing

$$S(\vec{p}, E)S(-\vec{p}, E) = G(0, 0; \vec{p}_{\|})\mathfrak{D}_\lambda(\vec{p}, E) \tag{2.27}$$

and

$$S(\vec{p}, E)\, e^{i\vec{p}\cdot\vec{R}_a} + (\vec{p} \to -\vec{p})$$
$$= [2\cos\vec{p}\cdot\vec{R}_a + e^{-\lambda} G(0, 0; \vec{p}_{\parallel})$$
$$\times \cos(\vec{p}\cdot\vec{R}_a + p_{\perp}a)]\mathfrak{D}_{\lambda}(\vec{p}, E) \,. \tag{2.28}$$

In the case of infinite damping, so that all emission is from the surface, we see

$$\mathfrak{D}_{\infty}(\vec{p}, E) = G(0, 0; \vec{p}_{\parallel}) \,. \tag{2.29}$$

Combining Eqs. (2.27) and (2.29), we see that for $\lambda = \infty$, an average of I_b over the surface Brillouin zone (rather than a spherical average) yields just the surface-layer contribution $\Delta\rho_0$. I_{ab} reduces to $\mathfrak{D}_{\infty}$ times $2\cos\vec{p}\cdot\vec{R}_a$; for large $\vec{p}\cdot\vec{R}_a$, this term will be highly oscillatory as one performs a spherical average, and hence will be relatively small, as suggested in connection with Eq. (2.18).

In the no-damping limit, we find after some albegra and use of the definitions in Eqs. (2.23) and (2.26b) that simply

$$\mathfrak{D}_0(\vec{p}, E) = (E - E_{\vec{p}})^{-1} \,, \tag{2.30}$$

indicating that I_b and I_{ab} become singular (i.e., of order $N_{\parallel}$) for the energy and lattice-momentum-conserving excitation process. In this regard, it is instructive to examine the corresponding expression for the clean-surface photoemission in the present framework:

$$\pi^{-1}\,\mathrm{Im}\sum_{m=0}^{\infty}\sum_{n=0}^{\infty}[G^0(m-n; \vec{p}_{\parallel}) - G^0(m+n+2; \vec{p}_{\parallel})]\, e^{-i(m-n)p_{\perp}a} \tag{2.31}$$

since parallel crystal momentum is a good quantum number. The summations over the bulklike term $G^0(m-n)$ gives a contribution of $\delta(E - E_{\vec{p}})$ *per layer*. In addition, there is the surface term

$$\pi^{-1}\,\mathrm{Im}\left(\frac{i}{\mu}\right)\left(\frac{\cos p_{\perp}a}{E - E_{\vec{p}}} + \frac{\sin^2 p_{\perp}a}{(E - E_{\vec{p}})^2}\right)$$
$$\equiv \pi^{-1}\,\mathrm{Re}\left[\mu^{-1}\frac{1 + \omega\cos p_{\perp}a}{(E - E_{\vec{p}})^2}\right] \tag{2.32}$$

arising from the presence of a finite cutoff at the lower limits of the sums. Finally, the summations over the reflected wave term $G^0(m+n+2)$ separate into the product of two geometric series and contribute

$$+\pi^{-1}\,\mathrm{Im}[G^0(1; \vec{p}_{\parallel})/2(E - E_{\vec{p}})] \,. \tag{2.33}$$

We thus find coherent effects in general when energy and lattice momentum are conserved.

The above discussion has invariably assumed that there is a single adatom sitting directly above a surface atom, i.e., in the atop position. Here we shall show how to treat other symmetry positions.

Suppose that the adatom now sits symmetrically between two substrate atoms, called 1 and 2. The hopping Hamiltonian generalizes to

$$-V_{1a}\sum_{\sigma}(c_{1\sigma}^{\dagger}c_{a\sigma} + \mathrm{H.c.}) - V_{2a}\sum_{\sigma}(c_{2\sigma}^{\dagger}c_{a\sigma} + \mathrm{H.c.}) \,. \tag{2.34}$$

By symmetry, $V_{2a} = V_{1a}$. Then performing the sum gives

$$-\sqrt{2}\,V_{1a}\sum_{\sigma}\left[\left(\frac{c_{1\sigma}^{\dagger} + c_{2\sigma}^{\dagger}}{\sqrt{2}}\right)c_{a\sigma} + \mathrm{H.c.}\right] . \tag{2.35}$$

The form of Eq. (2.35) assures the normalization of the orbital into which the adatom's electron hops. Note that the effective potential $V^B = \sqrt{2}\,V_{1a}$ is augmented by a factor of $\sqrt{2}$ over the hopping V_{1a},[23] while the effective substrate neighbor of the adatom (the group orbital to which it bonds) is

$$|1\rangle^B = (|1\rangle + |2\rangle)/\sqrt{2} \,. \tag{2.36}$$

Correspondingly, if the adatom sits symmetrically between four substrate atoms, in the centered position, at the apex of a pyramidal pentahedron, then $V^C = \sqrt{4}\,V_{1a}$ and

$$|1\rangle^C = \tfrac{1}{2}(|1\rangle + |2\rangle + |3\rangle + |4\rangle) \,. \tag{2.37}$$

Here 1, 2, 3, and 4 denote the four corners (substrate atoms) of the square at the base of the pyramid.

Using Eqs. (2.36) and (2.37) and the appropriate symmetries and invariances, we find

$$G_{11}^B = G_{11} + G_{12} \,;$$
$$G_{11}^C = G_{11} + 2G_{12} + G_{13} \,. \tag{2.38}$$

Inserting the appropriate G_{11}^X and V^X, $X = A, B, C$, into Eq. (2.1) yields the corresponding generalization.

Generalizations for the local $\Delta\rho$ require more definitions. The generalized 11 element of the T matrix is [cf. Eqs. (2.36) and (2.37)]

$$\mathcal{T}_X = V_X^2/(E - E_a - V_X^2 G_{11}^X) = V_X^2\,\mathcal{G}_{aa}^X \,, \tag{2.39a}$$

while for substrate site i

$$G_{i1}^B = (G_{i1} + G_{i2})/\sqrt{2} \tag{2.39b}$$

and

$$G_{i1}^C = \tfrac{1}{2}(G_{i1} + G_{i2} + G_{i3} + G_{i4}) \,. \tag{2.39c}$$

With X binding the Dyson's equation method for $\mathcal{G}$ between substrate sites generalizes Eq. (2.2c) to

$$\mathcal{G}_{ij}^X = G_{ij}^{[A]} + \mathcal{T}_X\, G_{i1}^X\, G_{1j}^X \,. \tag{2.40}$$

Further extensions to the photoemission formulas follow naturally as we shall sketch. Starting with Eq. (2.17), we see that the change in photoemission rate due to chemisorption depends ultimately on $\Delta\tilde{\rho}_{\mu\nu}$, which by separability depends only on $G_{1\mu}$ and $G_{1\nu}$. If we substitute G_{1j}^B for G_{1j}^A in Eq. (2.18) or Eq. (2.21), the factor $e^{i\vec{k}_{\parallel}\cdot(\vec{R}_j - \vec{R}_1)}$ is replaced by $2^{-1/2}(e^{i\vec{k}_{\parallel}\cdot(\vec{R}_j - \vec{R}_1)} + e^{i\vec{k}_{\parallel}\cdot(\vec{R}_j - \vec{R}_2)})$. If $\vec{R}_2 - \vec{R}_1$ is denoted by $a\hat{x}$, then the old exponential is modified by the inclusion of a new factor of the form

$$2^{-1/2}(1+e^{-ik_x a}) = 2^{1/2} e^{-ik_x a/2} \cos\tfrac{1}{2} k_x a \ .$$

Then the performance of the j summation produces a δ function between $\vec{k}_{\parallel}$ and $\vec{p}_{\parallel}$ as before. In angular-averaged Δj and in I_b, there will be the product of this term and its momentum-space inverse, so that the adatom sitting at a B site produces a factor of the form

$$2\cos^2\tfrac{1}{2} p_x a = 1 + \cos p_x a$$

in Eq. (2.22) or (2.19) (p_x being k_x in the latter). Similar arguments for centered binding generate a new factor of the form $(1+\cos p_x a)(1+\cos p_y a)$. These factors are just what one would expect from the discussion in ES.

III. COMPUTED RESULTS

A. Changes in density of states

In the following we shall take E_a to be near the center of the band, at -0.3 in energy units where the substrate nearest-neighbor hopping is $\frac{1}{2}$ and hence the bandwidth is 6. For E_a near the band center, reactivity is maximized, for a half-filled band, perhaps somewhat artificially so. But we will bring out the covalent aspects of the chemisorption process. Indeed, for our typical adsorbate, E_a as given by the average of the ionization and affinity levels is roughly 7 eV below the vacuum (cf., Table I) while the center of a nickel band is roughly 7 eV below vacuum (and for tungsten, it is 5 or 6 eV down), so that the ansatz may often be reasonable.

TABLE I. Collection of some relevant metallic and atomic-energy parameters (in eV).

bcc metals	Work function[a]	$W_b \sim E(H_{25'}) - E(H_{12})$	$E_F - E(H_{12})$
W $5d^5 6s^1$	4.5 ± 0.2	10.5 (14.1)[b]	6.2 (7.8)
Mo $4d^5 5s^1$	4.2 ± 0.2	9.2[b]	5–6
Cu $3d^5 4s^1$	4.6 ± 0.2	6.9[b,c]	4.4
Fe $3d^7 4s^1$	4.4 ± 0.2	4.9[c]	4.2
V $3d^4 4s^1$	4.1 ± 0.3	6.6[c]	3.3
fcc metals		$\sim E(X_7^+$ highest$) - E(X_6^+$ lowest$)$	$E_F - E(X_6^+$ lowest$)$
Ni $3d^9 4s^1$	5.0 ± 0.4	$4.8[E(X_5) - E(X_1)]$[c]	$4.7[E_F - E(X_1)]$
Pd $4d^{10}$	5.0 ± 0.5	5.9[d]	5.4
Pt $5d^9 6s^1$	5.4 ± 1.0	8.0[d]	7.0
Rh $4d^8 5s^1$	4.8 ± 0.2	7.3[d]	6.2
Ir $5d^7 6s^2$	4.9 ± 0.4	9.5[d]	7.7

"Covalent" adsorbate	Ionization potential (I)[a]	Affinity level (A)[a]	$\frac{1}{2}(I+A)$
H	13.595	0.75	7.2
O	13.614	1.47	7.5
O_2	12.063	0.44	6.3
N	14.53	<0	7.3
NO	9.25	0.91	5.1
CO	14.013	?	
C	11.256	1.25	6.3
F	17.418	3.45	10.4
S	10.357	2.08	6.2
Cl	13.01	3.81	8.3
Alkali adsorbate			
Li	5.4[a]		
Na	5.1		
K	4.3		

[a] Handbook of Chemistry and Physics, 52nd ed. (Chemical Rubber Co., Cleveland, Ohio, 1971).
[b] L. F. Mattheiss, Phys. Rev. 139, A1893 (1965).
[c] L. F. Mattheiss, Phys. Rev. 134, A970 (1964).
[d] O. Krogh Andersen, Phys. Rev. B 2, 883 (1970).

For a system of adatom plus substrate the $\Delta\rho$ gives the difference in distribution of wave-function energies for some finite V and the same system with $V=0$. In the laboratory, however, one measures the clean substrate, then allows adsorbate gas to enter, measures the adsorbed substrate, and finds the difference. Thus, we should investigate $\Delta\tilde{\rho}$, which augments $\Delta\rho$, the total DOS by the free-adatom DOS,

$$\Delta\tilde{\rho} = \Delta\rho + \delta(E - E_a) \qquad (3.1)$$

since there is just a single sharp orbital on our model adatom. Since we are adding an electron state to the system[24] (but using an off-diagonal perturbation), we find the sum rule

$$\int_{-\infty}^{\infty} \nabla\tilde{\rho}(E)\, dE = 1 \ . \qquad (3.2)$$

By examining $\Delta\tilde{\rho}$ we can gain some understanding of what happens during the process of chemisorption. For vanishing V, we find just a δ-function spike at E_a corresponding to the addition of an orbital to the system. As V becomes finite, we expect a second-order perturbation-theory repulsion between E_a and the levels of the bulk. Indeed, we find that the spike about E_a is broadened (and possibly also shifted) by an amount proportional to V^2. In this regime, which has been termed weak binding by Grimley,[10] the so-called virtual-level approximation is appropriate. This case is pictured in Fig. 1 for $V=\frac{1}{2}$.

As V increases, the $\Delta\tilde{\rho}$ curve continues to broaden and also to shift away from the band center toward the side on which E_a is. (For $E_a=-0.3$, the peak shifts down in energy.) But around $V=1$, the curve develops a shoulder on the other side of E_a. By $V=1\frac{1}{2}$, or moderate strength binding, we find (cf. Fig. 1) that the shoulder has developed into a second peak of roughly the same magnitude as the first. These two peaks correspond to bonding and antibonding resonances. The width of $\Delta\tilde{\rho}$, which runs roughly as the strength of the adatom-substrate bond, is now characterized by the separation of the two peaks rather than their individual widths. This separation goes more nearly like V than V^2. As V continues to increase, the peaks narrow and approach the band edge, splitting off from the band first on the side on which E_a is, then on the other, as illustrated in Fig. 1. These split-off states, which correspond to bonding and antibonding states, have unit weight. In order to satisfy the sum rule

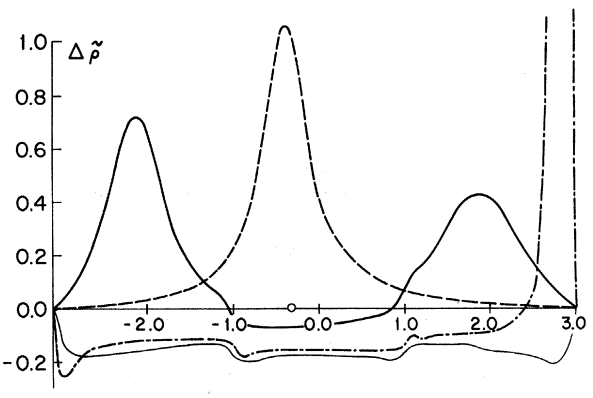

FIG. 1. Total change in density of states ($\Delta\tilde{\rho}$) vs energy for four adatom-substrate hopping strengths: $V = 0.5$ (dashed), 1.5 (heavy solid), 2.504 (dot-dashed), and 3.5 (light solid). The energy unit is one-sixth of the bandwidth. The adatom-level parameter E_a, indicated by the small circle on the abscissa, is -0.3 relative to the energy zero at the band center.

of Eq. (3.2) there must therefore be a region of negative $\Delta\tilde{\rho}$ in the center region of the band, which we indeed find. The physical interpretation of these curves is that the adatom and its nearest neighbor, called 1, on the surface combine to form a dimer-like structure referred to as a *surface complex*.[6,25] To free atom 1 to enter into the complex, however, we must first sever its bonds with its substrate neighbors. In forming an indented solid, we remove DOS from the center of the band region. By $V = 3\frac{1}{2}$, this picture is nearly achieved. The bonding split-off state lies roughly at $-V$ (at -3.84, for this V of $3\frac{1}{2}$), and the $\Delta\tilde{\rho}$ within the band region is qualitatively the same as that for the indented solid. Quantitatively, the $V = 3\frac{1}{2}$ $\Delta\tilde{\rho}$ is smaller in magnitude than the indented solid $\Delta\tilde{\rho}$ by of order 10% except near the edges. The extra negative $\Delta\tilde{\rho}$ near the edges in the $V = 3\frac{1}{2}$ case can be viewed as perturbational repulsion between the split-off states and the band, which disappears as these bonding-antibonding states get very far from the band. In summary, even though in adding an adatom electron to the system we expect the DOS to increase for all energies, we find that in fact it decreases near the band center for moderate to strong binding.

While Newns[6] has previously elaborated (graphically and analytically) on the emergence of split-off states, his linear model lacks three features of more general systems that the (100) sc lattice includes. We recall that a split-off state occurs when $E - E_a - V^2 g(E)$ vanishes outside the band, where $g(E) = \mathrm{Re}G^X(E)$ is the Hilbert transform of the DOS. If it vanishes within the band, and the DOS is relatively small, we find not a sharp state but a resonance.

Since Newns chooses to work with the analytically tractable semi-infinite chain, he has a semielliptical DOS. Consequently his $g(E)$ is just proportional to E within the band, allowing for only one zero within the band. However, for tight-binding models the one-dimensional bandwidth is $\frac{1}{3}$ that of the three-dimensional one. Indeed our $g(E)$ is roughly linear in E in the middle third of the band, but is decreasing in magnitude near the band edges, thereby providing the possibility of the intermediate regime.

Second, a linear-chain model does not permit any inclusion of steric effects. As we showed in Sec. II, it is easy to generalize our formalism to allow the adatom to sit symmetrically between two surface atoms in the bridge or B position or between four in a centered or C position (at the apex of a pyramid whose square base is formed by four surface atoms). The adsorption Hamiltonian automatically selects the bonding combination of the two or four relevant substrate atomic orbitals. By moment arguments[17] or otherwise, we see that these hybridized orbitals' DOS are narrowed and lowered in energy. Specifically, the peak position (first moment) and widths (second moment about this mean) for A, B, and C binding orbitals are 0, $-\frac{1}{2}$, and -1, and $\frac{5}{4}$, 1, and $\frac{3}{4}$, respectively. Figure 2 illustrates this discussion, showing how with the same parameters $\Delta\tilde{\rho}$ for C binding suggests a narrower, lower substrate band.

A final consequence of the linear-chain model is that the DOS has $(E - E_0)^{1/2}$ singularities near an edge E_0, rather than $(E - E_0)^{3/2}$ for the three-dimensional case.[8,9,26] This $\frac{1}{2}$ singularity is the same as one finds in the bulk case, and in a similar manner,

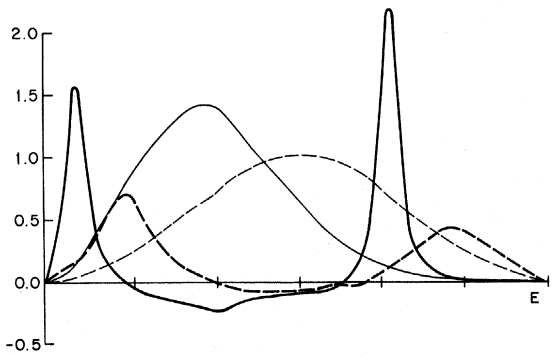

FIG. 2. Illustration of the effect of an adatom sitting at the four-fold centered (C) position (solid curves) rather than the atop (A) position directly over a substrate site. The light curves give π times the (unperturbed surface) DOS that the adatom electron encounters in hopping to the bulk, and shows that the C curve is shifted down and narrowed. The heavy curves give the resultant $\Delta\tilde{\rho}$ for $V = 1.5$ and $E_a = -0.3$; i.e., the heavy dashed curve gives the same quantity as the heavy solid curve of Fig. 1. The grid of the abscissa is the same as in Fig. 1.

we find that $g'(E)$ diverges as one approaches the band edge from outside, leading to a zero in a coefficient for the local DOS of a split-off state[27] and hence a delocalized state dramatically unlike the surface complex picture painted above.[26,28] This delocalization is consistent with the absence of bonding and antibonding resonances within the band.

How accurate is the name surface complex? How well are the electrons participating in the adatom-substrate band localized in that vacinity? Figure 3 shows the change in the local DOS for various sites near the adatom, using Eqs. (2.2c) and (2.4). Choosing to work with the hopping $V=1.5$ so that all relevant features are visible within the band, we find that the two-peak structure characterizing the surface complex appears only on the adatom and site 1, its nearest neighbor in the substrate. The peaks are completely absent from the nearest and next nearest neighbors of 1 on the surface. Furthermore, the $\Delta\rho$'s on these neighbors are sharply down from that on the adatom and site 1, and they are increasingly wiggly, rather like Friedel oscillations. The reason the peaks for the ρ_{aa} and $\Delta\rho_{11}$ curves are comparable is that E_a is near the band center. If E_a were well below it, then the bonding (antibonding) peak of ρ_{aa} ($\Delta\rho_{11}$) would be more pronounced than that of $\Delta\rho_{11}$ (ρ_{aa}); and vice versa, if E_a were above the center. Figure 3 also shows the unperturbed DOS of site 1. Adding to it $\Delta\rho_{11}$ verifies that ρ_{11} is non-negative throughout the band and that it essentially vanishes near the center, indicating a repulsion between E_a and the substrate levels or, viewed as an indentation process, a draining of the band states on the site to provide substance for the surface complex.

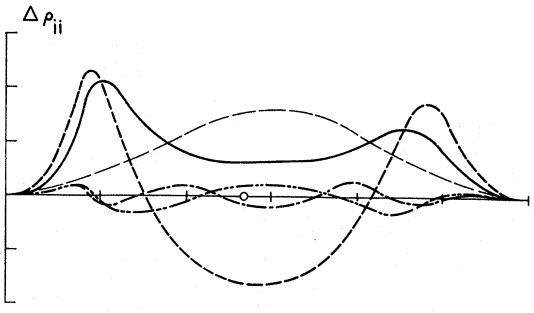

FIG. 3. Local DOS for the adatom (solid) in the atop position; and the local $\Delta\tilde{\rho}$ for the substrate atom directly beneath, called 1 (dashed), and a nearest (dot-dot dashed) and a next-nearest (dot-dashed) neighbor of 1 in the surface plane. Both axes are in the same units and are drawn to the same scale as Fig. 1; again E_a is -0.3 and $V=1.5$. In the background is ρ^0_{11} (light long-dashed curve), as appeared in Fig. 2. The positive-definite ρ_{11} is the sum of ρ^0_{11} and $\Delta\rho_{11}$.

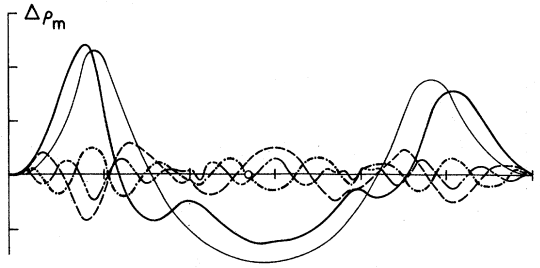

FIG. 4. Planar or subtotal $\Delta\tilde{\rho}$ for the top (heavy solid), second (dashed), third (dot-dashed), and fourth (solid double dashed) layers. The axis scales are identical to Figs. 1 and 3, the parameters V and E_a to Fig. 3. Included also is $\Delta\rho_{11}$ (light solid) to suggest the reliability of the surface-complex approximation.

As shown in Eq. (2.14) it is not difficult to sum the local $\Delta\rho$ within any layer. These $\Delta\rho_m$ are displayed in Figure 4 for the top four layers, again with $V=1\frac{1}{2}$. Again, the two-peak resonance structure with a depletion of states in the band center appears only for the top layer. The DOS in lower layers are much smaller in amplitude and are in-

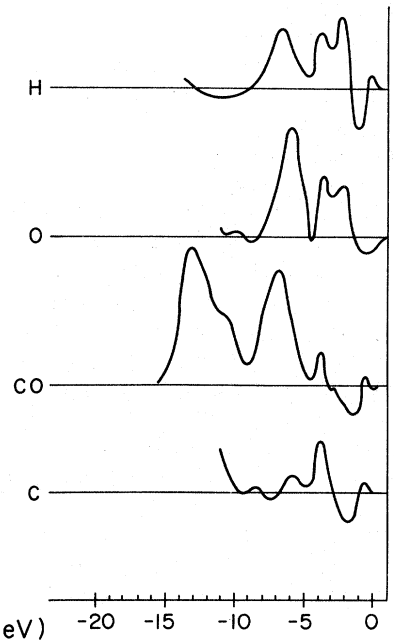

FIG. 5. Angular-averaged photoemission difference spectra in arbitrary intensity units for four adsorbate on (110) tungsten, as obtained by Plummer (Ref. 22). Energy is measured relative to the Fermi energy rather than the band center, and the abscissal energy unit is eV rather than bandwidth/6. The depletion region lies about 1 eV below E_F, while the bonding peak sits near the bottom of the band, around -6 eV.

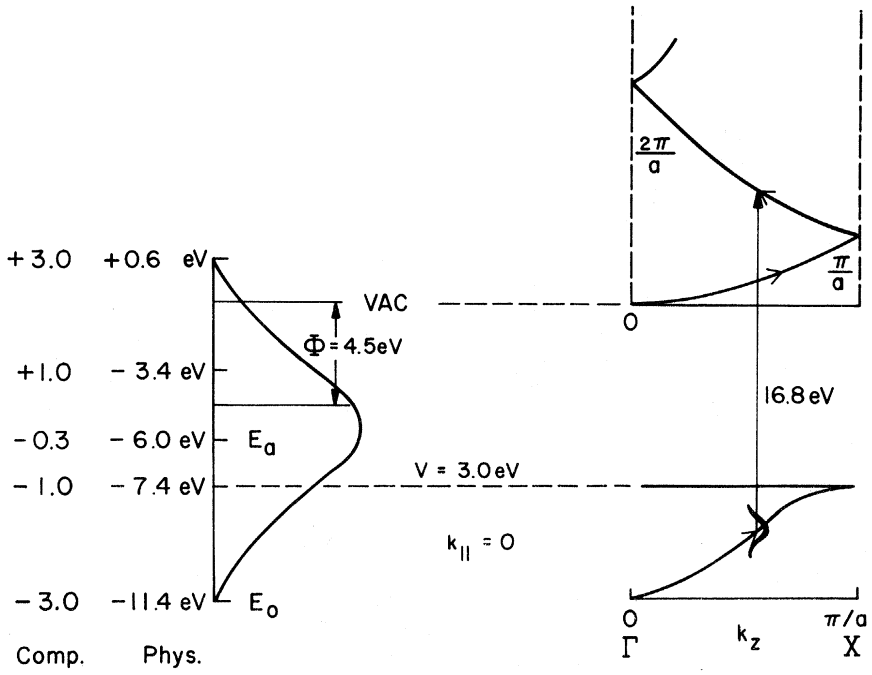

FIG. 6. Schematic drawing illustrating our simple view of normal (angular-resolved) photoemission from adsorbed tungsten. The substrate is represented by the (100) face of a sc lattice (surface DOS depicted) with bandwidth 12 eV (standard energy unit 2 eV), work function 4.5 eV, and center 5.4 eV below vacuum. Normal photoemission selects the lowest third of the band, and a one-dimensional cosine band structure. The 16.8-eV photons excite electrons into a plane-wave state with energy measured relative to the vacuum (no inner potential). Bulk emission is δ-function-like, conserving momentum. The presence of a surface smears the one-dimensional band. Finally, an adatom is placed in the atop position, with a V of 3 eV and E_a at 0.6 eV below the band center.

creasingly oscillatory. While the initial decrease in amplitude is marked, subsequent decay is only mild. The implication of these features for probes of the electronic surface structure is that for moderate or strong binding one should invariably see the bonding resonance (and also the antibonding one, if it is occupied), and a depletion of states near the band center. However, as the depth to which the probe is sensitive varies (e.g., by adjusting energy or angle to alter escape depth), the admixture of lower layers will change, resulting in a variable fine structure in the observed difference spectrum. Usually there will be additional sources of variable fine structure. Figure 4 includes $\Delta\rho_{11}$ from Fig. 3 to illustrate that the approximation of replacing $\Delta\tilde{\rho}$ by just $\rho_{aa}+\Delta\rho_{11}$ (here $\sum_i \Delta\rho_{ii}$ by $\Delta\rho_{11}$) is often reasonable, at least for gross features, as in the work of Gadzuk.[29]

B. Applications to photoemission

The two surface probes used most widely in studying the effect adsorption on DOS are field emission and ultraviolet photoemission.[22] The former, relying on a tunneling mechanism, is only sensitive to (i) a few eV below the Fermi level and (ii) the adatom and top layer. In the following we shall show how our model can give a general understanding of some of the features of photoemission difference spectra, that is the difference between a surface with an adatom bonded to it and a clean surface. In the formalism developed in Sec. II, we have made the rather drastic simplification of taking the final state to be just plane waves. Liebsch[20] discusses the effects of multiple scattering in the final state for a (100) sc lattice. In addition, we have omitted an inner potential to avoid an extra free parameter and refraction at the surface. An inner potential could be added without special difficulty, but we expect its inclusion to make no qualitative change.

As we saw in Eq. (2.18) and related discussion, we can roughly approximate the angular averaged change in photoemission yield by $\Delta\tilde{\rho}$, or more generally, by a layer sum with a damping factor added. Figure 5 illustrates experimental data by Plummer[22] for H, O, C, and CO on the (110) face of tungsten. From Table I, E_a as given by the negative average of the ionization and affinity levels is roughly 7 eV below vacuum, or $1\frac{1}{2}$ eV below the band center (or about $\frac{3}{4}$ in units of bandwidth/6), roughly where ours lies. The Fermi energy is about 1 eV ($\frac{1}{2}$ unit) above the band center, so that

the band is a bit more than half-filled. If moderately strong binding occurs, we expect the difference spectrum to show a depletion of states in the center of the band and the formation of a bonding peak near the bottom. These predictions are borne out in Fig. 5. No antibonding peak appears since the Fermi level lies below it. In Fig. 5, H and O have a similar characteristic structure in the range 2–5 eV below E_F. We have no satisfactory explanation of this similarity. The corresponding phenomenon for C and CO most likely arises from the apparent dissociation of CO when binding on W.[22] Moreover, since real substrates involve several orbitals per substrate site, and real adatoms often have more than one bonding orbital, one might often find more than one binding peak.

In an angular-resolved measurement with low damping, the spectrum will be dominated by the bulk excitation process that conserves normal crystal momentum in addition to energy and parallel momentum, as seen in Eq. (2.30). Surface terms

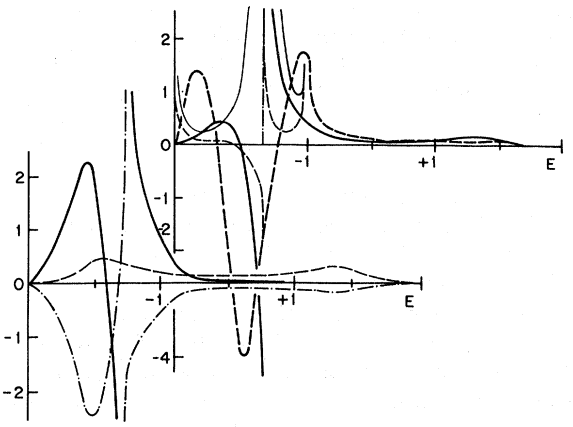

FIG. 7. Computed predictions for normal photoemission scenario of Fig. 6. All curves are concentrated in the lower third of the band, verifying the one-dimensional nature. In the upper plot, the vertical dash-dot line marks the position E_p of the bulk momentum-energy-conserving condition. The two light curves give the modification of δ-function behavior due to the presence of a (clean) surface: the solid line shows the effect of truncation of the layer sum, and the dashed line the role of the "reflected wave" produced by the boundary condition. Both have $(E-E_c)^{-1/2}$ singularities at the edge of the edge of the (one-dimensional) band and $(E-E_p)^{-1}$ singularities at E_p. The two heavy lines give the total change in rate in the limits of zero (solid) and infinite (dashed) damping, the latter corresponding to just the adatom and top layer. The structure of the undamped curve indicates an infinitesimal upward shift of the δ-function peak, suggestive of a repulsion between it and the bonding resonance. The lower plot decomposes the zero-damping curve into bulk (solid), adatom (dashed), and adatom-bulk interference (dast-dot) contributions. To grasp the scale, note that the adatom curve is the same as the ρ_{aa} curve of Fig. 3.

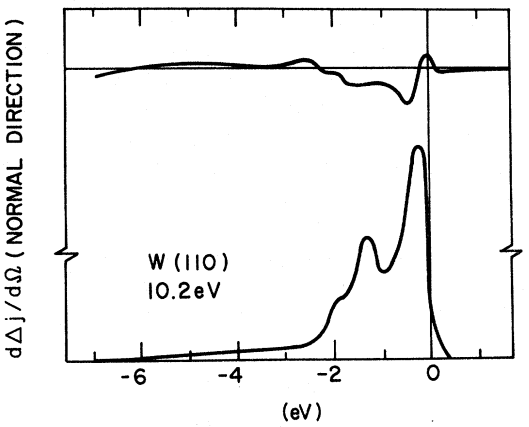

FIG. 8. Experimental data for normal photoemission from (110) tungsten, obtained by Feuerbacher and Fitton (Ref. 30) with 10.2-eV photons. The lower curve gives the clean-surface emission and shows the energy-momentum-conserving peaks dominating the spectrum. The upper curve gives the difference spectrum when 0.03 monolayer of hydrogen is allowed to adsorb on the surface. The characteristic trough-peak structure indicates a shifting up of the peak near E_F, their zero of energy, as in Fig. 7.

will broaden this sharp line. In the following we shall focus attention on photoemission in the direction normal to the surface. In this case, the inclusion of an inner potential would not produce a surface refraction effect on the final state plane wave. On the other hand, the fact that $\vec{k}_{\parallel}$ is zero leaves us with a one-dimensional DOS situated in the lowest third of the substrate band. Figure 6 depicts the highly simplified viewpoint we have chosen; Fig. 7 presents resulting calculational results based on Eqs. (2.20)–(2.23); and Fig. 8 shows the corresponding experimental information. As Fig. 6 suggests and Fig. 7 corroborates, in addition to broadening the sharp $\vec{k}$-conserving line, the surface terms will also exhibit $E^{-1/2}$ singularities at the one-dimensional zone boundaries, corresponding to the divergence of the inverse derivative of the cosine.

If chemisorption creates a bonding resonance below the broadened energy-momentum-conserving line, we would expect a perturbationlike repulsion between the two peaks, shifting the bonding resonance down slightly in energy while raising the $\vec{k}$-conserving peak infinitesimally. Such a shift in a large peak by a small amount is manifested by a trough-crest feature in a difference spectrum. In the limit of an infinite peak shifted infinitesimally, it becomes a line descending to $-\infty$ followed immediately by one dropping from $+\infty$. We see such behavior in Fig. 7 for an undamped process. For a damped process, and ultimately for emission from just the surface, this feature is muted, as il-

lustrated. From Eq. (2.20), it is natural to separate the contributions to the difference spectrum from the adatom, the bulk, and their interference. Thus, it would not be at all hard to include orbital dependence effects. Low-coverage data from Feuerbacher and Fitton[30] for H on W (110) displayed in Fig. 8 corroborates this dominance of the spectrum by the $\vec{k}$-conserving peak. There is a (bonding) peak at $2\frac{1}{2}$ eV below E_F; for correspondence with angular averaged data, we would expect one at about -6 eV. The experimental data do not go to this depth.

IV. SUMMARY AND DISCUSSION

In exploring the $\Delta\rho$ for an adatom on a (100) s-band simple-cubic lattice, we have seen how as the chemisorption strength increases, the bond changes from a perturbative broadening of the adatom level to a creating of a surface complex. This dimerlike structure is well localized in the band region. After considering steric effects, we applied our framework to photoemission difference spectra, where we could interpret the formation of a peak near the bottom of the band and the depletion of states near the Fermi level in terms of the surface complex.

In translating to actual systems, we would view carbon monoxide on nickel as an example of weak binding and oxygen on tungsten as an example of strong binding. While the s-band ansatz made analytic calculations possible, it hinders quantitative comparison with real systems. Thus, in CO adsorption, many levels shift; on the other hand, the 5σ level, which is localized near the carbon, shifts most dramatically, so that we might take its initial position as E_a. While O on W falls in to the surface-complex regime, the low-coverage desorption product is O rather than WO or some other oxide of tungsten.[31] This might be a consequence of an inadequate treatment of cohesion in the substrate, especially the neglect of multiple electrons in the d band. Alternatively, if O adsorbs in the centered position, the indentation process extracts a symmetric group orbital rather than an individual one; the chemisorption bond is clearly not strong enough to extract four substrate atoms. These cases show how our picture can be helpful in understanding chemisorption phenomena, but that one cannot apply it naively.

This paper has dealt exclusively with just one adatom on the surface, a picture which would be valid for a dilute adlayer. Often we find, however, that at low coverages the adatoms do condense into islands below some critical temperature. ES detailed how to understand the ordered layers in terms of an anisotropic oscillatory rapidly-decaying indirect interaction between adatom pairs. Figure 9 depicts the corresponding $\Delta\rho$ correction terms

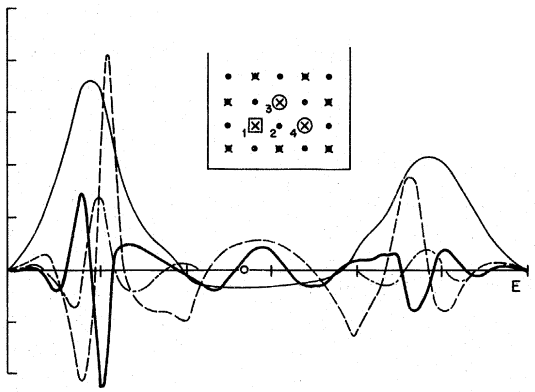

FIG. 9. Multiadatom corrections to the total $\Delta\tilde{\rho}$. The light solid curve repeats the $\Delta\tilde{\rho}$ vs energy for a single adatom in the atop position with $V=1.5$ and $E_a=-0.3$, as in Fig. 1, and with identical axis scales in Figs. 1, 3, and 4. The inset depicts a $c(2\times2)$ adlayer structure. The total $\Delta\tilde{\rho}$ due to the $1-3$, next-nearest neighbor (dashed) and $1-4$, next-next-nearest neighbor (dot-dashed) pair interactions—i.e., two adatoms nearby minus twice the single adatom result—are seen to be rather sizable but seem mostly to serve to split or fine tune the bonding and the antibonding resonances. Also plotted is the $\Delta\tilde{\rho}$ from the $1-3-4$ trio interaction (heavy solid), viz., adatoms on sites 1, 3, and 4 minus thrice the single atop adatom contribution and minus the three constituent pair terms.

that would arise from the pair interactions producing a c (2×2) structure, as well as a further correction due to the previously undiscussed three-adatom interaction.

The effects of these multisite terms are not as drastic as a first glance at Fig. 9 might suggest. Their magnitude is concentrated in the region of bonding and antibonding resonances. The sharp peak-trough character suggests they will shift and split the resonances. The corrections will be less important in computing interaction energies, since these involve essentially double integrals in energy over the DOS. Since the successive correction terms are not only smaller in amplitude (though not always to the point of negligibility) but also successively more oscillatory, their contributions at least to energetics should not be too significant. Further investigations of this area are in progress.

Although a detailed review is unwarranted here, we should say at least a word about the sort of corrections arising from self-consistency effects. In our model, V, E_F, and E_a can no longer be treated as independent parameters. We fixed the first two, then solved for E_a such that $n_{a\sigma}$ was $\frac{1}{2}$ (rather than using the Friedel sum rule).[32]

Qualitatively, our findings for a less than half-filled band are that excess charge will tend to accumulate on the surface complex to take advantage of the increased hopping V and the edgelike position. On

site 1, this pileup is seen explicitly, while on the adatom E_a moves up from E_F ($E_a = E_F$ starts the iteration) toward the center of the band. The excess charge drops off rapidly, at least initially, as we move away from the surface complex. The nearest-neighbor excess charge partially compensates (i.e., has the opposite sign of) the excess charge on atom 1. Also, the excess charge oscillates with E_F when we get to the next neighbor, and no doubt will fluctuate more rapidly with E_F as distance from the surface complex increases. (If we allowed a diagonal term on site 1, it would be negative for the clean surface[7,33] to compensate for band narrowing and would rise with chemisorption to prevent charge buildup near the bond.) We find substantial effects, though not as overwhelming as would be suggested by extensions to intermediate V of Allan's work at $V = \frac{1}{2}$. In any case, the perturbation is highly localized near the surface complex.[34]

ACKNOWLEDGMENTS

The author takes pleasure in thanking Professor E. Ward Plummer for suggesting this area of investigation, and for much encouragement and advice during the course of calculations. He is also very grateful to Professor J. Robert Schrieffer for several highly illuminating discussions and comments, and to him and to Dr. Robert H. Paulson for reading the manuscript and offering helpful suggestions. Conversations with Professors Paul Soven and Edward A. Stern were also very helpful, especially with regard to questions of self-consistency. Some of the final stages of this project were carried out at the Aspen Center for Physics.

---

*Work supported by the National Science Foundation and the Advanced Research Projects Agency.

†Present address: Dept. of Physics and Astronomy, University of Maryland, College Park, Md. 20742.

[1]R. Hoffmann, J. Chem. Phys. 39, 1397 (1963); 40, 2474 (1963); 40, 2480 (1963); A. J. Bennett, B. McCarroll, and R. P. Messmer, Surf. Sci. 24, 191 (1971); D. J. M. Fassaert, H. Verbeck, and A. van der Avoird, *ibid.* 29, 501 (1972); L. W. Anders, R. S. Hansen, and L. S. Bartell, J. Chem. Phys. 59, 5277 (1973); and Alfred B. Anderson and Roald Hoffmann, *ibid.* 61, 4545 (1974).

[2]J. A. Pople and D. L. Beveridge, *Approximate Molecular Orbital Theory* (McGraw-Hill, New York, 1970); A. J. Bennett, B. McCarroll, and R. P. Messmer, Phys. Rev. B 3, 1397 (1971); G. Blyholder, Surf. Sci. 42, 249 (1974).

[3]J. C. Slater and K. H. Johnson, Phys. Rev. B 5, 844 (1972); Phys. Today 27, (No. 10), 34 (1974) and listed references.

[3]N. D. Lang, Solid State Phys. 28, 225 (1973); N. D. Lang and W. Kohn, Phys. Rev. B 1, 4555 (1970); J. R. Smith, S. C. Ying, and W. Kohn, Phys. Rev. Lett. 30, 610 (1973).

[5]T. B. Grimley, Adv. Catal. Relat. Subj. 12, 1 (1960).

[6]D. M. Newns, Phys. Rev. 178, 1123 (1969).

[7]Guy Allan, Ann. Phys. (Paris) 5, 169 (1970).

[8]T. L. Einstein and J. R. Schrieffer, Phys. Rev. B 7, 3629 (1973).

[9]D. Kalkstein and P. Soven, Surf. Sci. 26, 85 (1971).

[10]T. B. Grimley, Proc. Phys. Soc. Lond. 90, 751 (1967); 92, 776 (1967); J. Vac. Sci. Technol. 8, 31 (1971); T. B. Grimley and S. M. Walker, Surf. Sci. 14, 395 (1969).

[11]D. Penn, R. Gomer, and M. H. Cohen, Phys. Rev. Lett. 27, 26 (1971); Phys. Rev. B 5, 768 (1972); D. Penn, Phys. Rev. Lett. 28, 1041 (1972).

[12]P. W. Anderson, Phys. Rev. 124, 41 (1961).

[13]T. L. Einstein, Surf. Sci. 45, 713 (1974).

[14]Our "clean" surface should not be confused with the "free" surface of spin-wave theory as discussed by Leonard Dobrzynski and D. L. Mills [Phys. Rev. 186, 538 (1969)]; D. L. Mills and A. A. Maradudin [J. Phys. Chem. Solids 28, 1855 (1967); and 30, 784 (1969)]; and R. F. Wallis, A. A. Maradudin, I. P. Ipatova, and A. A. Klochikhin [Solid State Commun. 5, 86 (1967)].

[15]J. W. Davenport, Proceedings of the 34th Annual Physical Electronics Conference, Bell Labs, 1974 (unpublished).

[16]J. W. Davenport, T. L. Einstein, and J. R. Schrieffer, Japn. J. Appl. Phys. Suppl. 2, 691 (1974).

[17]F. Cyrot-Lackmann, J. Phys. Chem. Solids 29, 1235 (1968).

[18]R. Haydock, V. Heine, and M. J. Kelly, J. Phys. C 5, 2845 (1972).

[19]T. L. Einstein (unpublished).

[20]A. Liebsch, Phys. Rev. Lett. 32, 1203 (1974); A. Liebsch and E. W. Plummer, J. Phys. C (to be published).

[21]Eugen Merzbacher, *Quantum Mechanics* (Wiley, New York, 1961), Chap. 19.4.

[22]E. W. Plummer, in *Topics in Applied Physics: Surface Physics*, edited by Robert Gomer (Springer-Verlag, Berlin, to be published); E. W. Plummer, B. J. Waclawski, and T. V. Vorburger, in Proceedings of the the 145th Meeting of the Electrochemical Society, San Francisco, May 1974 (unpublished).

[23]This augmentation of the potential was omitted in ES, Ref. 8. Its absence does not effect any of the conclusions, since ES do not make any claim of how V_{1a} varies with adatoms site X. We are grateful to Dr. M.-C. Desjonquères for pointing out the omission.

[24]Actually we are taking our isolated adatom to be "prepared" for restricted Hartree-Fock; it is doubly occupied (or vacant) if E_a is below (or above) the Fermi energy. To maintain symmetry in S_ϵ, the clean substrate, isolated adatom, and adsorbed system must all have an even number of electrons. The preparation effects can be included by hand, but they represent charge-transfer effects that contribute to the ionic aspect of the bond. Our interest here is to focus on the covalent effects, which go to zero as V^2 for small V.

[25]T. B. Grimley, J. Vac. Sci. and Technol. 8, 31 (1971); J. R. Schrieffer, J. Vac. Sci. Technol. 9, 561 (1972).

[26]F. Cyrot-Lackmann and M.-C. Desjonquères, Surf. Sci. 40, 423 (1973); F. Cyrot-Lackmann, M.-C. Desjonquères, and J. P. Gaspard, J. Phys. C 7, 925 (1974).

[27]Since $E - E_a - V^2 g(E)$ is the argument of the δ function coming from $\mathcal{G}$ (ultimately $\mathcal{G}_{aa}$) and producing the split-

off state, we get a factor of $|1-V^2g'(E)|^{-1}$ in front of $\delta(E-E_{\text{split-off}})$; cf. also Ref. 6.

[28]J. Friedel, F. Gautier, A. A. Gomes, and P. Lenglart, *Quantum Theory of Atoms, Molecules, Solid State* (Academic, New York, 1966), pp. 445.

[29]J. W. Gadzuk, J. Vac. Sci. Technol. 11, 275 (1974); Solid State Commun. 15, 1011 (1974); and Phys. Rev. B 10, 5030 (1974).

[30]B. Feuerbacher and B. Fitton, Phys. Rev. B 8, 4890 (1973).

[31]David A. King, Theodore E. Madey, and John T. Yates, Jr., J. Chem. Phys. 55, 3236 (1971).

[32]J. Friedel, Nuovo Cimento Suppl. 7, 287 (1958). As in ES and Grimley (Ref. 10), we can work in a framework in which electron number rather than chemical potential is fixed. The s-wave phase-shift sum rule is $\int_{-\infty}^{E_F}\Delta\rho(E)\,dE=-\Delta\,E_F\,\rho_0\,(E_F)$.

[33]G. Allan and P. Lenglart, Surf. Sci. 30, 641 (1972).

[34]J. Rudnick and E. A. Stern [Phys. Rev. B 7, 5062 (1973)] treat the analogous problem of a substitutional impurity in a bulk sc lattice. While claiming that nearest- and next-nearest-neighbor diagonal perturbations are needed and influence residual resistivity and specific heat, they find that these two energy parameters are two orders of magnitude smaller than that on the impurity.